nuclear fusion
IAEA

PAPER

Resonance broadened quasi-linear (RBQ) model for fast ion distribution relaxation due to Alfvénic eigenmodes

To cite this article: N.N. Gorelenkov *et al* 2018 *Nucl. Fusion* **58** 082016

View the article online for updates and enhancements.

Related content

- Validating predictive models for fast ion profile relaxation in burning plasmas
  N.N. Gorelenkov, W.W. Heidbrink, G.J. Kramer et al.
- Resonance frequency broadening of wave-particle interaction in tokamaks due to Alfvénic eigenmode
  G. Meng, N.N. Gorelenkov, V.N. Duarte et al.
- Energetic particle physics in fusion research in preparation for burning plasma experiments
  N.N. Gorelenkov, S.D. Pinches and K. Toi

Recent citations

- Study of the likelihood of Alfvénic mode bifurcation in NSTX and predictions for ITER baseline scenarios
  V.N. Duarte *et al*

This content was downloaded from IP address 192.188.106.50 on 10/07/2018 at 18:09

IOP Publishing | International Atomic Energy Agency Nuclear Fusion

Nucl. Fusion **58** (2018) 082016 (12pp) https://doi.org/10.1088/1741-4326/aac72b

Resonance broadened quasi-linear (RBQ) model for fast ion distribution relaxation due to Alfvénic eigenmodes

N.N. Gorelenkov[1], V.N. Duarte[1,2], M. Podesta[1] and H.L. Berk[3]

[1] Princeton Plasma Physics Laboratory, Princeton University, Princeton, NJ, 08543, United States of America
[2] Institute of Physics, University of São Paulo, São Paulo, SP, 05508-090, Brazil
[3] Institute for Fusion Studies, University of Texas, Austin, TX, 78712, United States of America

E-mail: ngorelen@pppl.gov

Received 3 December 2017, revised 16 May 2018
Accepted for publication 23 May 2018
Published 29 June 2018

Abstract

The burning plasma performance is limited by the confinement of the super-alfvénic fusion products such as alpha particles and the auxiliary heating ions capable of exciting the Alfvénic eigenmodes (AEs) (Gorelenkov *et al* 2014 *Nucl. Fusion* **54** 125001). In this work the effect of AEs on fast ions is formulated within the quasi-linear (QL) theory generalized for this problem recently (Duarte 2017 *PhD Thesis* University of São Paulo, Brazil). The generalization involves the resonance line broadened interaction of energetic particles (EP) with AEs supplemented by the diffusion coefficients depending on EP position in the velocity space. A new resonance broadened QL code (or RBQ1D) based on this formulation allowing for EP diffusion in radial direction is built and presented in details. In RBQ1D applications we reduce the wave particle interaction (WPI) dynamics to 1D case when the particle kinetic energy is nearly constant. The diffusion equation for EP distribution evolution is then solved simultaneously for all particles along the angular momentum direction.

We make initial applications of the RBQ1D to a DIII-D plasma with elevated q-profile where the beam ions show stiff transport properties (Collins *et al* (The DIII-D Team) 2016 *Phys. Rev. Lett.* **116** 095001). AE driven fast ion profile relaxation is studied for validations of the QL approach in realistic conditions of beam ion driven instabilities in DIII-D.

Keywords: Alfvénic eigenmodes, fast ion distribution, quasi-linear theory

(Some figures may appear in colour only in the online journal)

1. Introduction

Despite the significant progress in the modeling of energetic particle (EP) driven instabilities in tokamaks in recent years, we still lack the reliable quantitative and predictive capabilities for fast ion confinement [1, 4]. When the dominant mechanism for fast ion transport is diffusive, a promising reduced approach is the quasi-linear (QL) modeling which offers the advantage of a simplified, and therefore less computationally demanding framework [5, 6]. If the mediator of EP transport is a collective instability such as the Alfvénic eigenmode (AE) instability, the eigenmode structure and resonances are assumed to be fixed in time. Thus the modes can be treated perturbatively while the distribution function is allowed to evolve. For this reason the standard QL approach does not capture the instability frequency chirping or avalanches which are common Alfvénic spectral response that consist of fully nonlinear oscillations. We should note that a criterion for the likelihood of wave chirping onset (alternatively, a criterion for the non-applicability of the QL approach) has been recently derived and validated [7, 8], which verifies the application of the QL approach for practical cases.

While the conventional QL theory [5, 6, 9] only applies to the situations with multiple modes overlapping (i.e. when the Chirikov criterion [10] of resonance overlapping is satisfied), a line broadened quasi-linear model [11, 12] was designed to

 © 2018 IAEA, Vienna Printed in the UK

address the particle interaction with both isolated and overlapping modes. This is done by using the same structure of QL equations for fast ion distribution function (DF) but with the diffusive delta function broadened along the relevant path of resonant particles to produce a resonance line broadened quasi-linear (RBQ) diffusion. This is a key element of the RBQ model that the parametric dependencies of the broadened window reproduce the expected saturation levels for isolated modes.

The system of equations we use in the RBQ code was initially implemented for the case of the bump-on-tail configuration in Fitzpatrick's thesis [14]. Ghantous [15, 16] benchmarked this model with the Vlasov code bump-on-tail (BOT) [17] discussing regimes of its applicability. We revisit the RBQ model and modify it to the realistic cases of Alfvénic instabilities excited by the super-Alfvénic energetic ions for the first time. We express the RBQ equations in action and angle variables, and implement them within the NOVA/NOVA-K framework for subsequent TRANSP code simulations. Results are presented for a DIII-D discharge with the reversed shear safety factor profile and with elevated $q_{\min}$ values described recently [3, 18]. We show the predictive capability of the RBQ model and compare it with the results of the the kick model [19, 20].

This paper is organized as follows. The introduction is given in section 1. Then in section 2 we start the description of the RBQ formulation by prescribing the resonance line broadening in the Constants of Motion (COM) space to account for fast ion distribution function evolution near the resonances. Section 3 presents the RBQ system of differential equations written in flux and COM variables. Section 4 describes the adopted Probability Density Function (PDF) interface with the whole device modeling (WDM) prototype code TRANSP [21]. Then section 5 presents the RBQ results for selected DIII-D discharge. Finally section 6 summarizes the study and outlines future RBQ development.

2. Generalized resonance broadening framework

We introduce the QL model by describing first the resonance line broadening [22] which we make use of when building the RBQ code.

2.1. Resonance broadening and its parametric dependencies

Consider the wave particle interaction (WPI) resonance line broadening in two-dimensional space to investigate the problem of EP transport in the presence of realistic Alfvén eigenmodes. Assuming an interaction Hamiltonian in the form $e^{-in\varphi-i\omega t}$, the diffusion of a particle is along the paths of constant values of the expression

$$\omega P_\varphi + n\mathscr{E} = n\mathscr{E}' = \text{const}, \tag{1}$$

where ω and n are the angular frequency and toroidal mode number of the instability. If the diffusion is approximately along P_φ, i.e. at low mode frequency or high toroidal mode number, the whole problem can be reduced to the set of 1D ($\Delta\mathscr{E} \simeq 0$) equations as discussed in Fitzpatrick' s thesis [14]. The effect of several low-n modes on energetic particles cannot be determined without a code that captures the diffusion in full $\mathscr{E}, P_\varphi$ space. This is due to the complex particle dynamics in 2D space and possible resonance overlap [23].

The conventional collisionless QL diffusion set of equations in terms of action and angle variables can be expressed as [9]

$$\frac{\partial}{\partial t} f(\mathbf{J};t) = \frac{\partial}{\partial \mathbf{J}} \cdot \left[\underline{\underline{D}}(\mathbf{J};t) \cdot \frac{\partial f}{\partial \mathbf{J}} \right], \tag{2}$$

$$\underline{\underline{D}}(\mathbf{J};t) = \frac{2\pi}{M^2} \sum_k \frac{C_k^2(t)}{\omega_k^2} \sum_{\mathbf{l}} \mathbf{l}\mathbf{l} \delta\left(\mathbf{l}\cdot\boldsymbol{\omega_{AI}}(\mathbf{J}) - \omega_k\right) \alpha_{\mathbf{l}}^k(\mathbf{J}), \tag{3}$$

$$\frac{\mathrm{d}C_k^2(t)}{\mathrm{d}t} = 2\left(\gamma_{L,k} + \gamma_{d,k}\right) C_k^2(t), \tag{4}$$

$$\gamma_{L,k} = \frac{(2\pi)^3}{\omega_k M \delta K_k} \int \mathrm{d}\mathbf{J} \sum_{\mathbf{l}} \alpha_{\mathbf{l}}^k(\mathbf{J}) \left(\mathbf{l}\cdot\frac{\partial f}{\partial \mathbf{J}}\right) \pi\delta\left(\mathbf{l}\cdot\boldsymbol{\omega_{AI}}(\mathbf{J}) - \omega_k\right), \tag{5}$$

with index k denoting the mode of interest and structure contributions (often called matrix elements) are given by

$$\alpha_{\mathbf{l}}^k(\mathbf{J}) \equiv \left| \int \mathrm{d}\mathbf{x} \mathbf{e}_k(\mathbf{x},\omega_k) \cdot \mathbf{j}_{\mathbf{l}}{}^k(\mathbf{x} \mid \mathbf{J}) \right|^2,$$

where M is the resonant particle mass, $\mathbf{J} = (J_1, J_2, J_3)$ is the vector of actions of EP unperturbed motion (they can be substituted by COMs in NOVA notations $\mathscr{E}, P_\varphi, \mu$), f is the EP distribution function, $\underline{\underline{D}}$ is the EP diffusion coefficient matrix. ω_k, C_k and $\mathbf{e}_k$ are the eigenmode frequency, mode amplitude and the electric field structure. $\boldsymbol{\omega_{AI}} \equiv (\omega_{A1}, \omega_{A2}, \omega_{A3})$ is the canonical (action related) frequency vector containing the frequencies associated with the canonical angles and $\boldsymbol{l} = (l_1, l_2, l_3)$ is the vector of integer triad, $\gamma_{L,k}$ is the linear growth rate of the mode, $\gamma_{d,k}$ is the mode damping rate in the absence of the instability, δK_k is the wave energy (i.e., the full energy stored in a combination of fluid and field oscillations) normalized by C_k^2 and $\mathbf{j}_{\mathbf{l}}{}^k(\mathbf{x} \mid \mathbf{J})$ means the resonant particle current at radial point $\mathbf{x}$ and having an action $\mathbf{J}$ (both given in appendix A). The index k is a global identification of a mode while the index $\mathbf{l}$ is the set of indices that identifies a resonance. The resonance condition is represented by $\omega_k - \mathbf{l}\cdot\boldsymbol{\omega_{AI}}(\mathbf{J}) = 0$. In this paper we restrict the RBQ model to use $\boldsymbol{\omega_{AI}}(\mathbf{J}) = (\langle\omega_\varphi\rangle, \langle\omega_\theta\rangle, \langle\omega_c\rangle)$, where the vector components are the orbit-averaged toroidal, poloidal and cyclotron frequencies, respectively. Also, for this case, we restrict $\mathbf{l} = (n_k, -p, 0)$, where n_k is the toroidal mode number of mode k, p is an integer associated to a resonance $\mathbf{l}$ and the integer associated with the cyclotron motion is taken as zero since a low-frequency Alfvén wave is not able to achieve a cyclotron resonance. In the following we will use the resonance frequency notation:

$$\Omega_{\mathbf{l}}(\mathbf{J}) \equiv \mathbf{l}\cdot\boldsymbol{\omega}_{AI}(\mathbf{J}) \tag{6}$$

The QL theory assumes that the mode amplitudes remain small and therefore the theoretical coefficients are computed based on the unperturbed orbits. In conventional QL theory, particles are considered to be in resonance only if they exactly satisfy the wave resonance condition. This implies that resonant particles can only diffuse over the resonant point, which is clearly an ill-posed problem. Nonlinear effects, however, naturally broaden the resonances. Dupree [22] realized that the turbulent spectrum contributes to diffuse particle orbits away from their original unperturbed trajectories. In the RBQ model the resonant island width is incorporated into the QL theory in such a way that it reproduces the expected saturation levels for single modes from analytic theory [24]. The broadening itself introduces an additional nonlinearity into the problem. The resonance line is substituted by the broadening function $\mathscr{F}$ to replace the resonance delta function over the broadened width (see equation (8) and next section). The broadening function becomes a more realistic platform that allows the momentum and energy exchange between particles and waves [13].

In the RBQ model the window width is determined by the sum of three terms:

1. The net growth rate ($\gamma_k \equiv \gamma_{L,k} + \gamma_{d,k}$, where $\gamma_{L,k}$ and $\gamma_{d,k}$ are the linear (positive) growth and (negative) damping rates) as expected for the wave treated by ordinary quasi-linear theory. As long as the imaginary part of the frequency is accounted for, the diffusion coefficient naturally contains the Lorentzian (Cauchy) distribution which has the property of having the characteristic height of $1/\gamma_k$ and the full width equal to $2\gamma_k$ at half maximum. The broadening based on γ_k collapses to a delta function when $\gamma_k \to 0$, i.e. when the mode reaches saturation:
$$\pi\delta\left[\Omega_{\mathbf{l}}(\mathbf{J}) - \omega_k\right] \underset{\gamma_k\neq 0}{\to} \frac{\gamma_k}{\left(\Omega_{\mathbf{l}}(\mathbf{J}) - \omega_k\right)^2 + \gamma_k^2}.$$
2. The separatrix width expected for a wave treated by single mode theory. In the phase space, particles that exchange energy with the mode are trapped by the separatrix of width $4\omega_{b,\mathbf{l}}$ [13]. Each particle satisfy a nonlinear pendulum equation with a given bounce trapping frequency $\omega_{b,\mathbf{l}}$ (defined in equation 10) which leads to the phase mixing for a single wave.
3. The effective collisional frequency $\nu_{scatt,\mathbf{l}}$ (as defined in [25, 26], see equation (9)) since collisions imply that particles are redistributed, being kicked in and out of the separatrix, which leads to particle decorrelating from the resonance. This increases the effective range of the resonance region since more particles are allowed to interact with the mode via the resonant platform. The value of $\nu_{scatt,\mathbf{l}}$ is sensitive to the choice of the mode numbers and frequency.

The resonances are given by (see equation (6)) the value of the resonance frequency:

$$\Omega_{\mathbf{l}}(\mathscr{E}, P_\varphi, \mu) = n_k\left\langle\omega_\varphi(\mathscr{E}, P_\varphi, \mu)\right\rangle - p\left\langle\omega_\theta(\mathscr{E}, P_\varphi, \mu)\right\rangle = \omega_k, \tag{7}$$

where p is an integer, $\omega_\varphi \equiv \dot{\phi}$ and $\omega_\theta \equiv \dot{\theta}$ are the toroidal and poloidal precession frequency contributions. Here the $\Omega_{\mathbf{l}}$ specifies the integration path in NOVA-K formulation as described in [27] and in the appendix A. It has been found [14, 15] that the broadening width is

$$\triangle\Omega_{\mathbf{l}}(\mathscr{E}, P_\varphi, \mu) = a\omega_{b,\mathbf{l}} + b\left|\gamma_k\right|\{= \left|\gamma_{L,k} + \gamma_{d,k}\right|\} + c\nu_{scatt,\mathbf{l}}, \tag{8}$$

The numerical constants a, b and c follow from verification with analytic theory for the modal problem of single mode dynamics (see appendix B). The scattering and the bounce frequencies can be expressed as follows [26]:

$$\nu_{\mathrm{scatt},\mathbf{l}} \simeq \nu_\perp R^2\left\langle v^2 - v_\parallel^2\right\rangle\left(\left.\frac{\partial\Omega_{\mathbf{l}}}{\partial P_\varphi}\right|_{\mathscr{E}}\right)^2, \tag{9}$$

$\nu_\perp$ is the 90° pitch-angle scattering rate, $\langle\rangle$ is the drift orbit average, and

$$\omega_{b,\mathbf{l}} = \left|2C_k(t)V_{\mathbf{l}}(I_r)\mathbf{l}\cdot\left.\frac{\partial\Omega_{\mathbf{l}}}{\partial\mathbf{J}}\right|_{\mathbf{J}=\mathbf{J}_r}\right|^{1/2}, \tag{10}$$

where the subscript r denotes the resonant location in the phase space.

3. RBQ system of equations

For the single mode WPI case, the particle diffusion can be projected onto the most relevant 1D path for EP dynamics in the phase space which occurs for the constant values of the magnetic moment μ and $\mathscr{E}'$. Thus it is convenient to define the following differential operator that is essentially a gradient operator projected onto this path:

$$\frac{\partial}{\partial I} \equiv \mathbf{l}\cdot\frac{\partial}{\partial\mathbf{J}} = \omega\frac{\partial}{\partial\mathcal{E}} - n\frac{\partial}{\partial P_\varphi} = \omega\left.\frac{\partial}{\partial\mathcal{E}}\right|_{P'_\varphi} = -n\left.\frac{\partial}{\partial P_\varphi}\right|_{\mathcal{E}'}. \tag{11}$$

Then, the 1D RBQ equations can be written as

$$\frac{\partial f}{\partial t} = \frac{\partial}{\partial I}\left(\sum_{n_k,p,m,m'} D(I;t)\right)\frac{\partial f}{\partial I} + \left(\left|\frac{\partial\Omega_{\mathbf{l}}}{\partial I}\right|_{I_r}\right)^{-2}\nu^3_{scatt,\mathbf{l}}\frac{\partial^2(f - f_0)}{\partial I^2} \tag{12}$$

where

$$D(I;t) = \pi C_k^2(t)\,\mathcal{E}^2\frac{\mathcal{F}_{\mathbf{l}}(I - I_r)}{\left|\frac{\partial\Omega_{\mathbf{l}}}{\partial I}\right|}G^*_{m'p}G_{mp}, \tag{13}$$

and the matrices G are defined in appendix A.

The growth rate is given by (see appendix A)

$$\gamma_{L,k} = \frac{2M^2\pi^3 c}{z\omega_k \int \rho\,|\xi_k|^2\, d\mathbf{r}} \sum_{\sigma_\parallel} \int dP_\varphi d\mu d\mathcal{E} \sum_{m,m',p} G^*_{m'p} \mathcal{E}^2 \tau_b \frac{\partial f}{\partial I} G_{mp} \frac{\mathcal{F}_\mathbf{l}(I - I_r)}{\left|\frac{\partial \Omega_\mathbf{l}}{\partial I}\right|}, \tag{14}$$

where z is the EP electric charge ξ is the fluid displacement, and τ_b is the drift orbit period. The full system of RBQ equations is comprised by (4), (12), (14) and (8).

In equation (14) the delta function integration used in NOVA-K (see equation (A.1)) is substituted with the broadening window function $\mathcal{F}_\mathbf{l}(I - I_r)$. The region of integration, or broadening region, was introduced above at equation (8).

The derivatives $\partial\Omega_\mathbf{l}/\partial I$ are provided by NOVA-K. The broadening of the resonance can be performed by choosing $\mathcal{F}_\mathbf{l}$ as the **window function** with the width ΔI that satisfies $\int_{-\infty}^{\infty} \mathcal{F}_\mathbf{l} dI = 1$. The function $\mathcal{F}_\mathbf{l}$ can be arbitrarily chosen. It can, for example, be a flat top, a Gaussian shaped or perhaps even specified via the Dupree's window shape [22], which for the BOT case can be transformed to 1D window function across the resonance

$$\mathcal{F}_{\mathbf{l},\mathrm{Dupree}} = \mathrm{Re} \int_0^\infty \mathrm{d}t \exp\left[\mathrm{i}\,(\Omega_\mathbf{l} - \omega_k)\, t - D\left(\frac{\partial \Omega_\mathbf{l}}{\partial I}\right)^2 t^3/3\right]. \tag{15}$$

For the results reported in this paper we are employing a simple flat-top window function. An attempt to simulate the realistic window function is undertaken with some preliminary results recently reported [13]. An important question remains about the practical (theoretical and numerical) confirmation of such studies including the D and $\mathcal{F}_\mathbf{l}$ dependencies and anomalous pitch angle scattering.

3.1. Discretized equations and boundary conditions

Although in principle one can arbitrarily discretize the system of equations to solve them numerically, there are some restrictions that are implied by physical considerations. In order to conserve the system momentum (i.e. particle plus wave momenta) at all times, the discretized equations must guarantee internal self-consistency by adopting the time flow presented in [2]. This flow is chosen in such a way that both particle diffusion and mode amplitude evolution are calculated using the same window function at each time step.

The linear system matrix can only be inverted (and therefore the system can only be solved) when boundary conditions are added to the discretized system of equations. The code needs to account for a loss boundary in the $\mathscr{E}, P_\varphi$ plane that is different for each $\mu = \mathrm{const}$ slice. A Neumann-type condition specifies the values that the derivative of the distribution function takes at the boundaries of the domain. It imposes a constant flux $\Gamma = -D\partial f/\partial P_\varphi$ at the edge. Normally in the steady state this is associated with the reflective boundary conditions, when $D\partial f/\partial P_\varphi = 0$. On the other hand, the Dirichlet-type boundary condition imposes a constraint on the value of the function itself, such as at the loss cone when its value is mediated by the diffusion when we set up $f = 0$.

In our diffusion solver to relax the EP distribution function, we have the option to use either Neumann or Dirichlet boundary conditions. They are chosen based on the following physical arguments. At the loss boundary, f should be zero and Dirichlet is physically appropriate since it allows for particle loss. On the other hand for the inner regions of the plasma the resonant particles are allowed to accumulate and a Neumann condition describes the relevant physics (it is equivalent to a reflective condition, i.e. with zero net flux). Particle number over the plasma volume is automatically preserved if particles do not escape at the ends. However if particles reach the ends where they are unconfined the particle loss is quantifiable.

4. Probability density function interface with whole device modeling

We integrate the RBQ simulations in its present version into the transport code TRANSP which can be viewed as a prototype of the WDM code. It enables the time-dependent integrated simulations of a tokamak discharge. The code can be used to interpret existing experiments as well as to develop new scenarios or make predictions for future devices (e.g. ITER). For NB-heated discharges the NUBEAM module within TRANSP models the evolution of the energetic particle population based on neoclassical physics [21, 28]. Coulomb collisions, slowing down and charge-exchange events are modeled based on a Monte Carlo approach. To account for resonant fast ion transport induced by Alfvénic and other MHD instabilities, NUBEAM has been updated to include the physics-based reduced model, known as kick model [19, 20].

For NUBEAM calculations the kick model prepares the transport probability matrix, $p(\Delta\mathscr{E}, \Delta P_\varphi | \mathscr{E}, P_\varphi, \mu)$, for each instability or a set of instabilities to be included in simulations. The matrix is defined in COM variables in both RBQ and NUBEAM codes. For each COM grid point (or bin) in the phase space, $p(\Delta\mathscr{E}, \Delta P_\varphi)$ represents the probability of $\mathscr{E}$ and P_φ changes (kicks) experienced by the energetic ions as a result of their interaction with the instability.

In previous works [20, 29, 30] the transport probability matrices were computed numerically by the guiding center code ORBIT [31] using the mode structures from the NOVA code (details on how the matrix is computed for a given instability are found in the appendix of [20]). In this work the quasi-linear diffusion coefficient computed by the RBQ1D code is used instead to reconstruct the $p(\Delta\mathscr{E}, \Delta P_\varphi | \mathscr{E}, P_\varphi, \mu)$ probabilities under the assumption of negligible energy variations induced by the wave-particle interactions.

Consider the trajectory of a resonant particle subject to constraints in the $(\mathscr{E}, P_\varphi, \mu)$ space [32, 33]. Equation (1) implies that for a single mode the variations in $\mathscr{E}$ and P_φ are related through

$$\Delta P_\varphi / \Delta\mathscr{E} = n/\omega. \tag{16}$$

Based on this constraint and under the assumption of diffusive transport (implied by the RBQ1D formulation), the bivariate PDF for $\Delta\mathscr{E}$ and ΔP_φ changes can be represented as:

$$p\left(\Delta\mathscr{E},\Delta P_\varphi|\mathscr{E},P_\varphi,\mu,|C_k\mathbf{e}_k|\right)=p_0 e^{-\left[\frac{(\Delta\mathscr{E}-\Delta\mathscr{E}_0)^2}{\sigma^2_{\mathscr{E}}}+\frac{\left(\Delta P_\varphi-\Delta P_{\varphi 0}\right)^2}{\sigma^2_{P_\varphi}}-2\rho\frac{(\Delta\mathscr{E}-\Delta\mathscr{E}_0)(\Delta P_\varphi-\Delta P_{\varphi 0})}{\sigma_{\mathscr{E}}\sigma_{P_\varphi}}\right]/2(1-\rho)}, \tag{17}$$

with the normalization factor

$$p_0=\frac{1}{2\pi\sigma_{\mathscr{E}}\sigma_{P_\varphi}\sqrt{1-\rho^2}}. \tag{18}$$

The correlation parameter $\rho=\frac{\langle(\Delta\mathscr{E}-\Delta\mathscr{E}_0)(\Delta P_\varphi-\Delta P_{\varphi 0})\rangle}{\sigma_{\mathscr{E}}\sigma_{P_\varphi}}$ accounts for the coupling between $\Delta\mathscr{E}$ and ΔP_φ (expressed in equations (1) and (16)) which is defined for each mode by its frequency and toroidal mode number. The angular brackets indicate an average over the distribution function over the specific $(\mathscr{E},P_\varphi,\mu)$ bin. Note that the offset (or convective) terms $\Delta\mathscr{E}_0$ and $\Delta P_{\varphi 0}$ are vanishing for the cases when there is no systematic drift in energy or P_φ. The variances $\sigma_{\mathscr{E}}$ and σ_{P_φ} are related to the diffusion coefficients in energy and canonical angular momentum, $D_{\mathscr{E}}$ and D_{P_φ}, and give the spread of the distribution along the $\Delta\mathscr{E}$ and ΔP_φ axes:

$$\sigma^2_{\mathscr{E}}=4D_{\mathscr{E}}\delta t;\ \sigma^2_{P_\varphi}=4D_{P_\varphi}\delta t \tag{19}$$

which allows the computation of the transport probability matrix over the time step δt associated with resonant particles for known quasi-linear diffusivities from the RBQ1D model.

We note that in our applications the size of COM bins for NUBEAM is much larger than the grid size used in RBQ (and in NOVA-K) code, which was 200 points in P_φ by 150 points in λ and by 40 points in v directions respectively. We used the definition $\lambda=\mu B_0 E$ where B_0 is the magnetic field strength on the axis. Several grid points are combined into one bin for PDF of NUBEAM computations. The variances $\sigma_{\mathscr{E}}$ and σ_{P_φ} and the correlation parameter ρ are computed for each bin.

In general, the probability matrix from equations (17)–(19) corresponds to the WPI contribution to the total transport probability. Another term accounts for the fact that not all particles in a specific $(\mathscr{E},P_\varphi,\mu)$ bin are necessarily resonant with a given instability. In fact, there can be large portions of phase space where no resonances are present. In general, for each discrete $(\mathscr{E},P_\varphi,\mu)$ bin there is a fraction k_{res} of resonant particles and a fraction $k_{\text{non-res}}$ of unperturbed, non-resonant particles that are not affected by the instability. To compute those fractions one can infer the volume V_{res} occupied by resonant ions within the $(\mathscr{E},P_\varphi,\mu)$ bin and compute the ratio with respect to the total bin volume V_{tot}:

$$\begin{aligned}k_{\text{res}}\left(\mathscr{E},P_\varphi,\mu\right)&=\frac{V_{\text{res}}\left(\mathscr{E},P_\varphi,\mu\right)}{V_{\text{tot}}\left(\mathscr{E},P_\varphi,\mu\right)};\ k_{\text{non-res}}\left(\mathscr{E},P_\varphi,\mu\right)\\&=1-\frac{V_{\text{res}}\left(\mathscr{E},P_\varphi,\mu\right)}{V_{tot}(\mathcal{E},P_\varphi,\mu)}\end{aligned} \tag{20}$$

The values of k_{res} and $k_{\text{non-res}}$ depend on the resonant ion position in COM space and the sizes of used bins. In the case presented in the next section (figure 3(*b*)) they change from $k_{\text{res}}=0, k_{\text{non-res}}=1$ in the upper right corner of the figure (*b*), where no resonances are present, to $k_{\text{res}}\simeq 1, k_{\text{non-res}}\simeq 0$ near the midpoint in P_φ direction and low particle energies which are heavily populated by the resonances. In that figure the broadening across the resonance is proportional to the resonant ion volume V_{res}.

Once these two fractions are known for each bin the total probability is

$$\begin{aligned}p\left(\Delta\mathscr{E},\Delta P_\varphi\right)=\ &k_{\text{non-res}}\delta\left(\mathrm{I}-\mathrm{I}_{\text{bin}}\right)\\&+k_{\text{res}}p_{\text{res}}\left(\Delta\mathscr{E},\Delta P_\varphi|\mathscr{E},P_\varphi,\mu\right)\end{aligned} \tag{21}$$

with $\delta(\mathrm{I}-\mathrm{I}_{\text{bin}})$ being the delta function for a given bin, I_{bin} being the COM location of the center of the bin and p_{res} is defined in equation (17).

We have outlined above the computations of PDF matrices for fast ion diffusion in COM space for subsequent NUBEAM calculations. The formulation is presented in a general form implying the QL diffusion in both EP energy and canonical momentum directions. The results are obtained using the 1D version of the RBQ code and are described next.

5. Applications to critical gradient DIII-D experiments

We are choosing recent DIII-D experimental studies for RBQ application with the goal of performing initial validations. In those experiments several ubiquitous EP transport responses were recognized: (i) EP transport suddenly changes at bifurcation; (ii) the transport is intermittent in time; (iii) EP profiles are resilient to the changes in neutral beam injection (NBI) [3]. The AE power spectrum increases linearly with the total driving beam power above EP threshold level. One representative discharge is chosen, #159243, with 6.4 MW of tangential beam power for our analysis. The NBI application was modulated by a small amount, on average by 10% of its total power with 50% duty cycle. The NBI injection energy was 70 keV. One time slice is studied extensively, $t=805$ ms, when the reversed shear magnetic safety factor profile minimum value turns lower than $q_{\min}=3$. Its spectrogram is depicted in figure (1).

An interesting feature of the data was revealed later when the velocity space resolution allowed the demonstration of a rather unexpected hollow profile of EP distribution function. The data was collected in part by the Fast Ion D_α (FIDA) diagnostics with some velocity space resolution. A similar feature was found using the interpretive kick model where the integration of the EP distribution function was implemented along the same

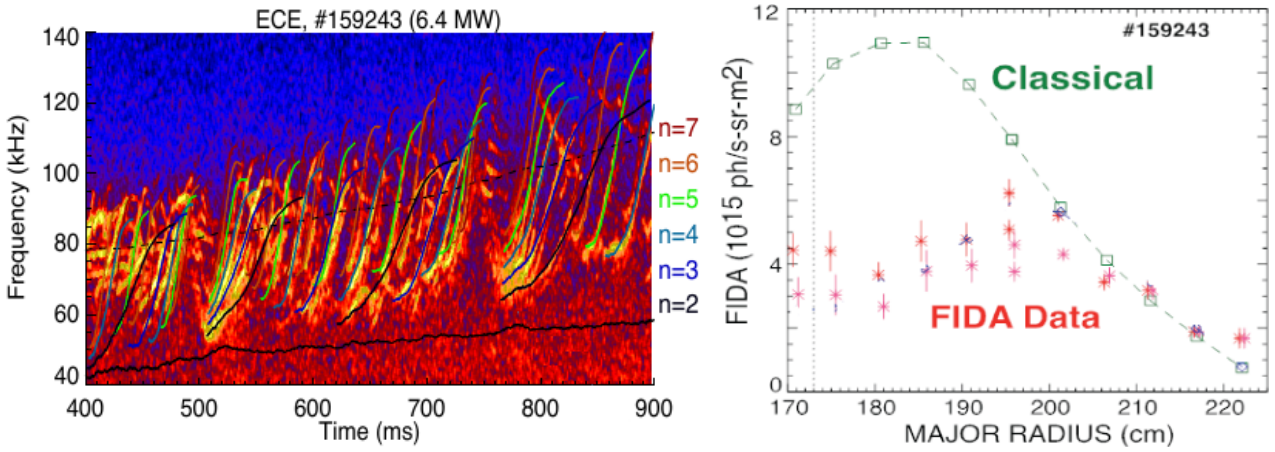

(a) (b)

Figure 1. A CO_2 interferometer power spectra for DIII-D shot #159243 during the current ramp with 6.5 MW NBI. The spectrum on figure (*a*) shows multiple sweeping frequency Reversed Share AEs (RSAE) and steady Toroidicity-induced AE (TAE) modes. Figure (*b*) compares classical TRANSP predictions for beam ion profile. The graph shows the error bar uncertainty associated with the background subtraction. The two sets of data represent two different light calibrations. The dotted vertical line indicates the location of the magnetic axis. Reproduced from [18], with the permission of AIP Publishing.

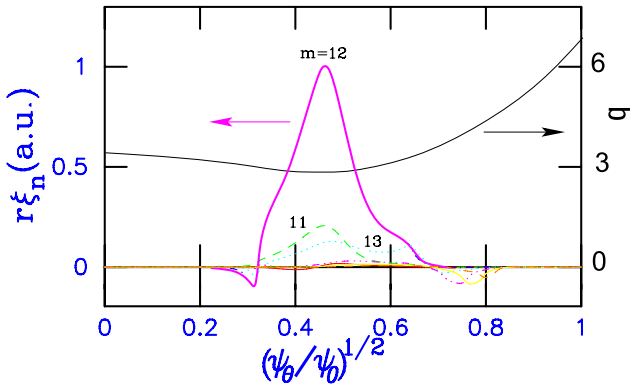

Figure 2. A plot of the q-profile of the plasma and spatial structure of poloidal harmonics for the radial displacement $n = 4, f = 84$ kHz RSAE computed by the ideal MHD code NOVA at 805 ms. The mode structure is computed for the plasma equilibrium with the shown safety factor profile. ψ_θ/ψ_0 is the poloidal flux normalized to its value at the wall.

FIDA 'view' window COM path. An application of the critical gradient model [34] to the same case did not find any hollow EP profile behavior but rather monotonic radial EP profiles.

5.1. Perturbative NOVA simulations for RBQ

Since RBQ is essentially perturbative and works as a postprocessor for NOVA/NOVA-K runs, its analysis is initiated by identifying the mode structures of AE instabilities responsible for EP transport. Extensive efforts were already undertaken with the kick model applications recently [18]. We make use of these RSAE/TAE results.

To show the details of RBQ analysis we take one of 11 experimentally measured modes, a $n = 4$ RSAE from [18] The mode is localized near $q_{\min} \simeq 3$ at $t = 805$ ms surface and has one dominant $m = 12$ poloidal harmonic which is shown in figure 2. Most of the measured modes are localized near $q_{\min}$ surface. Even though the modes are narrow in radius, fast ions from near the center can reach and interact with the AE modes very efficiently. In addition to the mode we show, there were several global TAEs with the spacial structure reaching the plasma edge.

The ideal MHD NOVA mode structures are used by the NOVA-K code [27] to evaluate the wave particle interaction (WPI) matrices for further processing by the RBQ code as described in section 2 and the appendix A. For the RSAE shown in figure 2, NOVA-K computes the normalized growth rate $\gamma_L/\omega = 3.2\%$ and the total damping rate $\gamma_d/\omega = -1.8\%$. The value of the damping rate is computed by the NOVA-K code. For relatively low toroidal mode number, n, it includes accurately dominant damping rate mechanisms: thermal ion and electron Landau dampings, trapped electron collisional damping which were benchmarked within the ITPA group recent activity [35]. Computed growth and damping rates for the modes of interest are typically consistent with observations and indicate that the AE instability is above or near the instability threshold.

The application of the NOVA-K code to DIII-D plasma of interest confirms the near threshold instability conditions of the observed RSAEs and TAEs. We rely on the RBQ formulation in that regime, i.e. the code computes the EP phase space diffusion coefficients (for the subsequent use of TRANSP) assuming that all the observed AEs are in the saturated states. These saturated states are either interpreted or predicted as far as AE amplitude is concerned. The corresponding broadening coefficients a, b, c of equation (8) are taken from [15].

As a result the broadening of the resonance line is computed at each resonance point within the RBQ code as illustrated in figure 3. Figure 3 (*a*) shows 7 resonance lines at one value of $\lambda = 0.4$ corresponding to co-passing. Figure 3 (*b*) shows the broadening of those resonances due to the first and the last terms in equation (8).

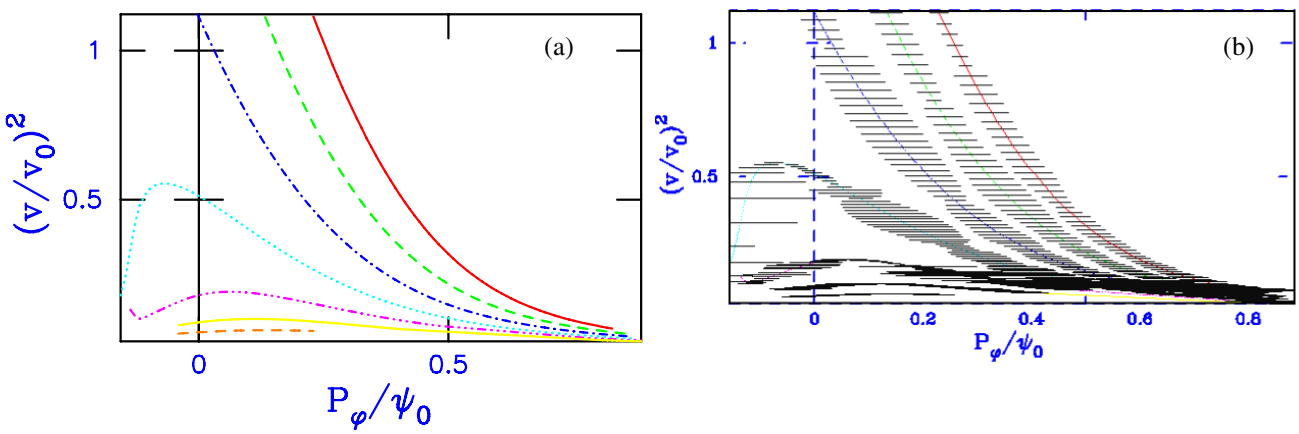

Figure 3. Resonance lines of passing EPs interacting with the RSAE mode (the mode structure is shown in figure 2) in the COM plane: normalized kinetic energy verusu canonical toroidal momentum. Shown in figure (*a*) are seven dominant resonances at $\lambda = 0.4$. Figure (*b*) represents the broadening of the resonance lines in the direction of P_φ computed at the mode amplitude $\delta B_\theta/B = 1.7 \times 10^{-3}$. ψ_0 is the poloidal flux at the wall divided by 2π and v_0 is the NBI ion speed at the injection.

The methodology to compute the broadening goes back to earlier publications on NOVA-K [26, 27]. The resonant frequency of the fast ion is computed by summing all the contributions from the ion precession frequencies as seen from equation (6) (see also equation (3) of [26]). The computed dependencies of $\Omega_{\mathbf{l}} = \omega_k$ for $n = 4$ mode in the COM space are shown in 3 (*a*). Each resonant particle due to several factors mentioned above experiences drift precession near the resonance point. The precession accounts for the broadening in P_φ direction according to equation (8).

The values of the frequencies in that equation, $\omega_{b,\mathbf{l}}$ and $\nu_{\mathrm{scatt},\mathbf{l}}$, are computed by NOVA-K code perturbatively for each resonance point and transferred to RBQ as a set of matrices. Once they are known (as well as the resonance frequencies $\Omega_{\mathbf{l}}$ and $\partial\Omega_{\mathbf{l}}/\partial P_\varphi$) the code finds the broadening of each resonance in P_φ direction: $\Delta P_\varphi = \Delta\Omega_{\mathbf{l}}/\left(\partial\Omega_{\mathbf{l}}/\partial P_\varphi\right)$.

The relaxation of EP distribution function (DF) can be computed within the RBQ simulations accurately. However in the present form the RBQ1D code computes the WPI induced diffusion into the TRANSP code through the probability density function (PDF) introduced above (see section 4 and also [36]). At the moment we will limit the initial RBQ1D application to such interface with TRANSP.

It has been shown that the kick model captures the EP diffusion in the velocity space which is substantially different from the diffusion 'ad hoc' model used normally in TRANSP and is a significant factor affecting the EP distribution function [29]. We employ the AE driven PDFs computed by RBQ within TRANSP and show the obtained results in the next figure 4. The results are for the single RSAE shown in figure 2.

Comparing three cases in the figure 4 tells us that the effect of AEs is similar on the beam ions if modeled by RBQ1D or by the kick models. Insert (*a*) tells us that most of the losses are at the low energies, $E_b = 10$–30 keV. This is consistent with the figure 3(*b*) which shows that this is where the resonances are most overlapped which results in stronger radial transport.

RBQ has been implemented in a way which allows either interpretive or predictive analysis. Let us consider them both.

5.2. Interpretive RBQ implementation for TRANSP code

The present mode of RBQ operation relies on AE amplitude values inferred from the experimental measurements. As we mentioned above, the kick model has been successful describing DIII-D FIDA experiments by computing EP diffusion specific to particle position in the COM space [18]. It reproduced the hollow EP pressure profiles as a result. We use the same amplitude values for RBQ1D analysis.

Details of TRANSP computations using PDFs are already published [20, 29, 30], so that here we present the results using those techniques. We add the RBQ prescribed PDFs and summarize this exercise in figure 5. The NBI power modulation is reflected in the neutron flux time evolution shown in figure 5(*a*) (and figure 6(*a*)).

One can see that both models work well by computing beam ion hollow density profiles. We should add however that in the interpretive mode RBQ1D and kick models had additional constraint due to the neutron flux.

Additional studies were done which show the origin of the inverse profile behavior. We have found that the origin of the reversed profiles is due to the diffusion of co-passing beam ions subject to strong diffusion. They are dominating the EP population near the center and are preferentially transported in radial direction outward.

5.3. Predictive RBQ implementation for TRANSP code

In the predictive RBQ analysis we repeated computations from the previous section 5.2 by using the same set of AEs. However we compute AE amplitudes in a different manner by finding their values when the particular mode reaches the saturation, i.e. when the growth rate balances the damping rate, $\gamma_{L,k} = -\gamma_{d,k}$.

In terms of the presented RBQ formulation in this paper this predictive case means the following. When we apply each mode separately within RBQ we adjust the amplitude of that mode in such a way that the mode amplitude is in the saturated state, i.e. the RHS of equation (4) is zero. That means

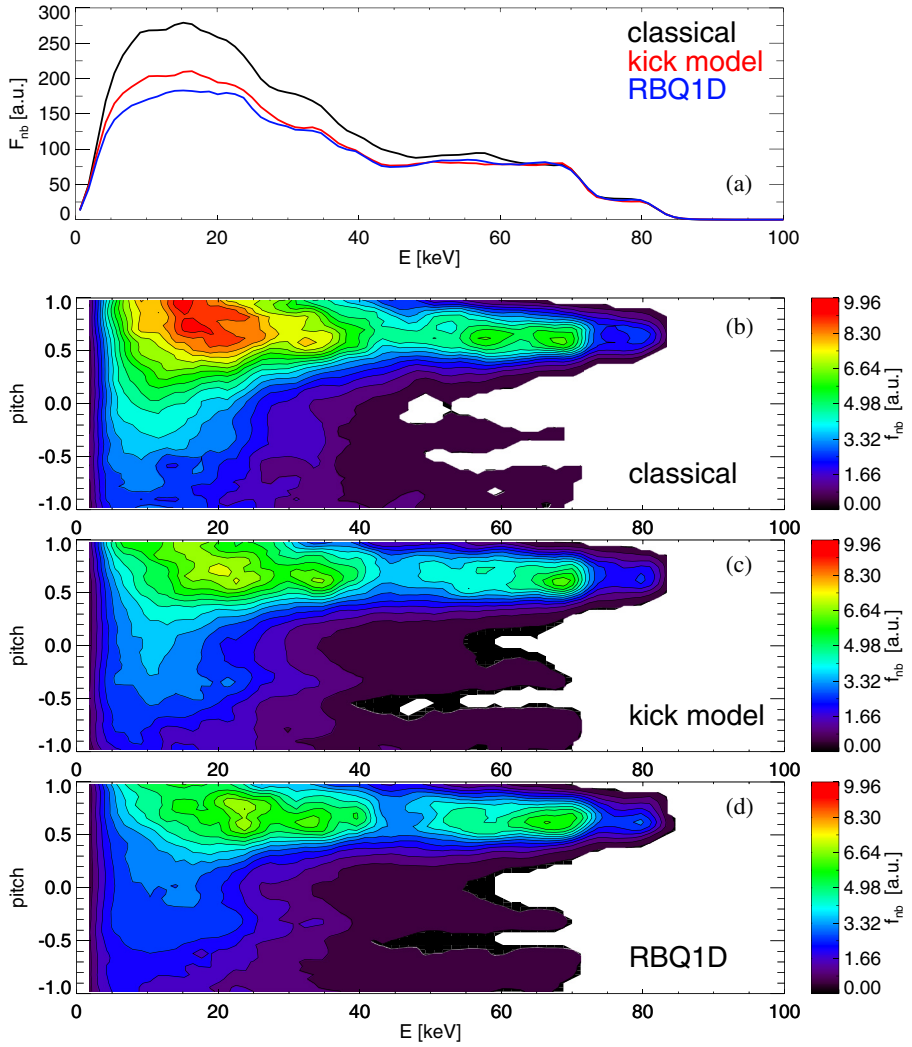

Figure 4. TRANSP simulated EP distribution function in the velocity space for the time of interest, $t = 805$ ms using the diffusion computed by RBQ1D and the kick model as indicated. Shown are DF averaged between the normalized poloidal flux $\sqrt{\psi/\psi_w} = 0.4$ and 0.6 values, where ψ_w is the poloidal magnetic field flux at the wall. Figure (*a*) shows the pitch angle averaged DF velocity dependence. Figures (*b*)–(*d*) correspond to the classical, kick model and RBQ1D simulations of the EP diffusion.

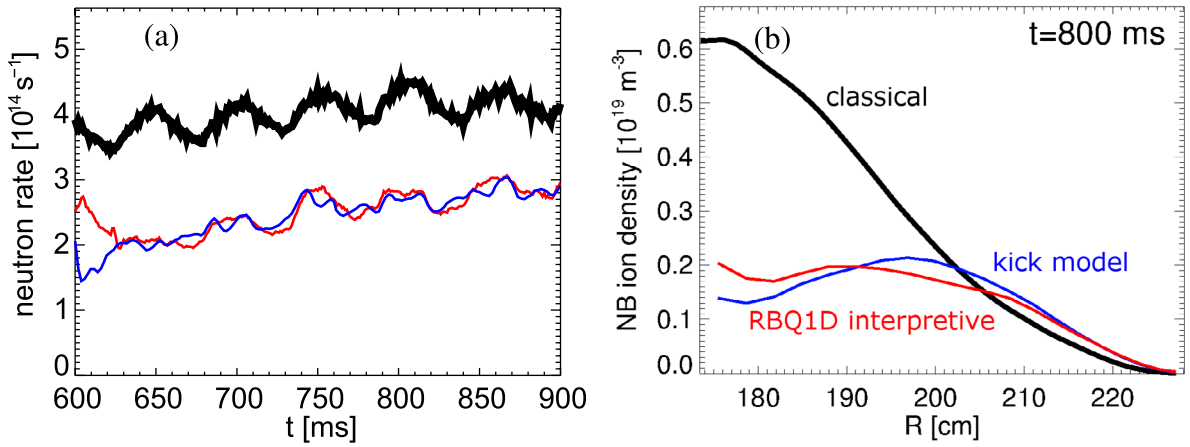

Figure 5. The left figure compares the neutron rate computed by TRANSP using various assumptions about EP diffusivities. Top (black, classical) dependence is obtained ignoring EP diffusion where the NBI was modulated by a small amount, on average 10% of its total power. Kick model fast beam ion density profiles are blue curves whereas RBQ1D profile and time dependencies are shown in red.

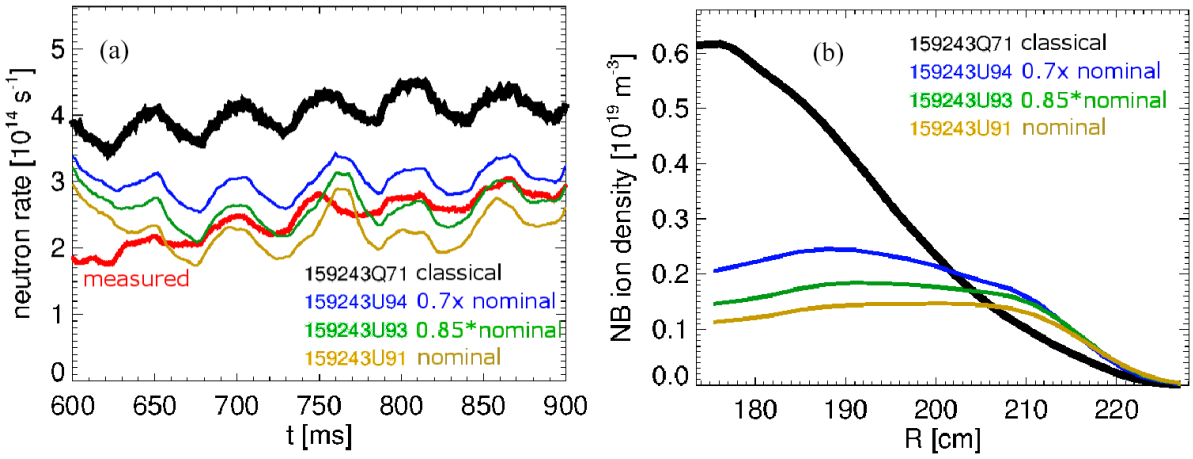

Figure 6. The same as in figure 5 but computed within the predictive TRANSP analysis. Different EP profile and evolution curves are color coded as indicated on the figure.

that the fast ion distribution function is relaxed to the state when the growth rate, equation (14), decreases to the level of the damping rate. The initial growth rate for each considered AE is computed by the NOVA-K code (see equation (A.1)) using the TRANSP computed EP distribution function when there is no EP diffusion due to the Alfvénic modes. Whereas the relaxed DF of the saturated state of the system defines the relaxed, saturated growth rate determined by equation (14).

This way we are not addressing the intermittency in AE transport seen in experiments (see figure 1), nor do we address the long time scale changes in AE stability as the RSAEs, for example, are sweeping its frequency on a hundred millisecond time scale.

The application of the predictive RBQ simulations within TRANSP are summarized in figures 6. After TRANSP turns the AE diffusion on at $t = 600$ ms the diffusion coefficients are kept constant throughout simulations. Figure 6 shows that the neutron deficit inferred by TRANSP-based analysis, would be replicated by RBQ for an AE amplitude that is 0.85 times its predicted value. The beam density profiles remains hollow within the amplitude variations.

6. Summary and future plans

This paper demonstrated the effectiveness of the quasi-linear model in its applications for realistic simulations of the beam ion self-induced relaxation via the Alfvénic instabilities. We have summarized the formulation for the Resonance Broadened QL (RBQ) numerical model with the EP diffusion near the resonances. The formulation can be applied for isolated or for the overlapping modes.

The RBQ1D has been applied in the interpretive and in the predictive modes to DIII-D critical gradient experiments via prescription of the PDF for beam ions. Initial results show that the model is sound and ready to be applied to predict the fast ion relaxation in burning plasmas. However more validations are required in order to gain the confidence in its predictive capability.

Among the immediate plans we have the development of the RBQ in its 2D version where the EP diffusion paths are sensitive to AE toroidal mode number and its frequency. The number of refined grid points of energetic particle diffusion and the need to resolve the resonances make the 2D problem intrinsically complex and computationally demanding.

Acknowledgments

This manuscript has been authored by Princeton University under Contract Number DE-AC02-09CH11466 and by DIII-D National Fusion Facility under Contract Number DE-FG02- 95ER54309 with the US Department of Energy and by the São Paulo Research Foundation (FAPESP, Brazil) under grants 2012/22830-2 and 2014/03289-4. The United States Government retains and the publisher, by accepting the article for publication, acknowledges that the United States Government retains a non-exclusive, paid-up, irrevocable, world-wide license to publish or reproduce the published form of this manuscript, or allow others to do so, for United States Government purposes.

We thank Dr. R. Nazikian for motivating valuable discussions.

Appendix A. Linear growth rate as a result of the nonadiabatic component of the distribution function

NOVA [27, 37] is a nonvariational, ideal MHD code primarily used to integrate non-Hermitian eigenmode equations in the presence of EPs, using a general flux coordinate system. NOVA-K [38] is a stability code used to study the destabilization of AEs by EPs free energy stored in the gradients of the distribution. The resonance response of energetic particles enter the system through the perturbed pressure associated with them. NOVA makes no use of inverse aspect ratio approximation and hence is well suited to study spherical tokamaks. The code uses Fourier expansion in θ and cubic spline finite elements in the radial ψ direction. Following the procedure of Cheng [38] we may start with the MHD formalism where the fast particle contribution is treated perturbatively, with all perturbed quantities represented in the form

$$A_k(\boldsymbol{r},t)=\sum_m A_m e^{i(S_m-\omega_k t)};\quad S_m\equiv m\theta-n_k\varphi.$$

We shall start with the momentum conservation equation. This equation can be put in a quadratic form if dot multiplied by $\boldsymbol{\xi}_k^*$ and integrated over the whole plasma volume. If equations (3.15) of [27] are used we get

$$D_k(\omega)=\delta W_{f,k}+\delta W_{h,k}-\delta K_k=0$$

where the inertial (kinetic) energy is given by $\delta K_k=\omega_k^2\int\rho|\boldsymbol{\xi}_k|^2\,d\mathbf{r}$. $\delta W_{f,k}$ is the total fluid potential energy and $\delta W_{h,k}$ is the EPs potential energy[4]. $\omega_k\delta W_{h,k}$ is the power being released by the resonant particles. The quadratic form is particularly useful when stability analysis is addressed. For example, if the mode frequency is assumed to be $\omega=\omega_k+i\gamma_{L,k}$, with $|\gamma_{L,k}|\ll|\omega_k|$, it is obtained [38]

$$\gamma_{L,k}\approx\frac{\Im\delta W_{h,k}}{2\delta K_k}\omega_k.$$

In the last equation, it was used that the inertial energy, δK_k, is close to the fluid eigenmode potential energy, $\delta W_{f,k}$. This is because Alfvén waves involve negligible electric field perturbations. Their energy is nearly equally divided between the perturbed magnetic energy and the kinetic energy of particles oscillating as a result of the perturbation. $\Re$ and $\Im$ denote the real and imaginary parts, respectively. $\delta K_k=\omega_k^2\int\rho|\boldsymbol{\xi}_k|^2\,d\mathbf{r}$ accounts for all poloidal harmonics and is simply a number, being a global factor for each toroidal mode number n_k. Since ρ is the total plasma density, it is very little affected by the fast ions density. This number is also provided by NOVA-K. For AEs, the growth rate is not simple as in the case of an idealized bump-on-tail configuration, being an integral over the resonant curve in phase space and depending on the mode structure. In order to compute $\Im\delta W_{h,k}$, and consequently $\gamma_{L,k}$, the non-adiabatic part of the distribution function, g, must be calculated. This function can be redefined as $\hat{g}$ to satisfy

$$\frac{d\hat{g}}{dt}=\frac{z}{M}\frac{\partial f}{\partial\mathcal{E}}(\omega_k-\omega_{*,k})\hat{X}$$

where $\omega_{*,k}=n_k(\partial f/\partial P_\varphi)/(\partial f/\partial\mathcal{E})$ is the diamagnetic frequency, being a measure of the relation of the radial gradient in the energetic in EP profiles to the velocity gradient. Since $\mathrm{d}P_\varphi=-\frac{qr}{\omega_c}\mathrm{d}r$ and the EP density decreases with radius, we have $\frac{\partial f}{\partial P_\varphi}>0$. On the other hand, the average energy of EPs also decreases with radius, which implies $\frac{\partial f}{\partial\mathscr{E}}<0$. Therefore, in a tokamak, the free energy stored in the radial gradient drives the mode while the negative gradient in energy tends to stabilize the mode. The mode is unstable when $\omega_{*,k}>\omega_k$ given by

$$\hat{X}=\left(\frac{\mathrm{d}\mathbf{r}_c}{\mathrm{d}t}-v_\parallel\hat{b}\right)\cdot J_0\nabla\phi_c+\frac{i\mu\omega_k M}{z}\frac{\mathrm{d}f}{\mathrm{d}\mu}(J_0+J_2)B_{\parallel c}$$

[4] In NOVA-K, both potential and kinetic energies are defined as twice their actual values. This can be seen from comparing equations (3.69) and (3.70) of [38] with equations (4.19) and (4.31) of [41]. This choice does not introduce changes to the growth rate.

where z is the EP charge and the subscript c mean that the quantity is evaluated at the particle gyrocenter. The Bessel functions are understood to have the argument $v_\perp\nabla_\perp/\omega_c$, which operates on the perturbed quantities. $v_\perp\nabla_\perp/\omega_c\sim v_\perp k_\perp/\omega_c\ll1$ which justifies the Taylor expansion of the Bessel functions, $J_\alpha(v_\perp\nabla_\perp/\omega_c)\to\sum_{j=0}^{\infty}\frac{(-1)^j}{j!\Gamma(j+\alpha+1)}(v_\perp\nabla_\perp/\omega_c)^{2j+\alpha}$. If $\mathbf{E}_{\perp,k}=-\nabla\phi_k$($\mathbf{A}_{\perp,k}$ contribution neglected) we can write

$$\hat{X}\simeq\frac{i\omega_k M}{z}\left[(2\mathcal{E}-3\mu B)J_0\boldsymbol{\kappa}\cdot\boldsymbol{\xi}_{\perp,k}-\mu BJ_0\nabla\cdot\boldsymbol{\xi}_{\perp,k}\right]$$

where $\boldsymbol{\kappa}$ stands for the curvature. The solution of the drift kinetic equation can be written as

$$\hat{g}=\frac{z}{M}\int^t\frac{\partial f}{\partial\mathcal{E}}(\omega_k-\omega_{*,k})\hat{X}\mathrm{d}t'$$

where the time integration is along the particle trajectory. Assuming $S_m(t=0)=0$, one can write in terms of the following Fourier series

$$\hat{X}=\sum_{m,p}e^{-i\omega_k t+i\overline{\omega}_{Dm}t}X_{mp}e^{ip\omega_\theta t}$$

$$X_{mp}=\frac{1}{\tau_b}\oint\mathrm{d}t'\hat{X}e^{i\int^{t'}(\omega_{Dm}-\overline{\omega}_{Dm}-p\omega_\theta)\mathrm{d}t''}$$

$\Im\delta W_{h,k}$ can then be calculated from

$$\delta W_{h,k}=-\int\int\hat{g}\mathbf{v}\cdot(\mathbf{v}\cdot\nabla)\xi_k^*\mathrm{d}\mathbf{r}_c\mathrm{d}\mathbf{v}=-\frac{\mathrm{i}z}{\omega_k}\int\int\hat{X}^*\hat{g}\mathrm{d}\mathbf{r}_c\mathrm{d}\mathbf{v}.$$

The phase-space integration is given by

$$\int d\Gamma...=\int d\mathbf{J}\int d\boldsymbol{\Theta}...=(2\pi)^3\int d^3J\sum_p...$$

$$=\int d\mathbf{r}_c\int d\mathbf{v}...=(2\pi)^2\sum_{\sigma_\parallel}\frac{B}{\omega_c}\int dP_\varphi\int d\mu\int d\mathcal{E}\int\mathrm{d}t...,$$

with $\mathrm{d}t$ being associated to the fast particle orbital motion. The integrals over φ and θ_g will contribute with 2π each. Note that in NOVA, P_φ, $\mathscr{E}$ and μ are defined without the mass. If they had usual units, we would have $\int\mathrm{d}\mathbf{r}_c\int\mathrm{d}\mathbf{v}...=(2\pi)^2\left(\frac{c}{zM^2}\right)\sum_{\sigma_\parallel}\int\mathrm{d}P_\varphi\int\mathrm{d}\mathscr{E}\int\mathrm{d}\mu\int\mathrm{d}t...$. We can write

$$\hat{g}=\frac{iz}{M}\sum_{m,p}\frac{e^{-i\omega_k t+i\overline{\omega}_{Dm}t+ip\omega_\theta t}}{\omega_k-\overline{\omega}_{Dm}-p\omega_\theta}\frac{\partial f}{\partial\mathcal{E}}(\omega_k-\omega_{*,k})X_{ml}.$$

Therefore

$$\delta W_{h,k}=-\frac{(2\pi M)^2c\omega_k}{z}\sum_{\sigma_\parallel}\int dP_\varphi d\mu d\mathcal{E}dt$$

$$\sum_{m,m',p,p'}G_{m'p}^*\frac{\mathcal{E}^2\left(\frac{\partial f}{\partial\mathcal{E}}\right)(1-\omega_{*k}/\omega,k)}{\omega_k-\overline{\omega}_{Dm}-p\omega_\theta}G_{mp}e^{-it\left(\overline{\omega}_{Dm'}-\overline{\omega}_{Dm}+(p'-p)\omega_\theta\right)}$$

where the 'drift' frequency is $\omega_{Dm}\equiv\frac{\mathrm{d}S_m}{\mathrm{d}t}$ and $\overline{\omega}_{Dm}$ means orbit averaged drift frequency, The matrix elements are defined as $G_{ml}=-\mathrm{i}\frac{zX_{ml}}{\omega_k M\mathscr{E}}$. The Plemelj formula could be used to develop the denominator. So, the imaginary part of $\delta W_{h,k}$ becomes

$$\Im\delta W_{h,k} = \frac{(2M)^2 \pi^3 c\omega_k}{z} \int dP_\varphi d\mu d\mathcal{E} \sum_{m,m',p} G^*_{m'p} \mathcal{E}^2 \tau_b \left(\frac{\partial f}{\partial \mathcal{E}}\right) \left(1 - \omega_{*,k}/\omega_k\right) G_{mp} \delta\left(\omega_k - \overline{\omega}_{D0} - p\omega_\theta\right).$$

The growth rate in NOVA is then given by:

$$\gamma_{L,k} = \frac{2M^2\pi^3 c}{z \int \rho \left|\boldsymbol{\xi}_k\right|^2 d\mathbf{r}} \sum_{\sigma_\parallel} \int dP_\varphi d\mu d\mathcal{E} \sum_{m,m',p} G^*_{m'p} \mathcal{E}^2 \tau_b \left(\frac{\partial f}{\partial \mathcal{E}} - \frac{n_k}{\omega_k} \frac{\partial f}{\partial P_\varphi}\right) G_{mp} \delta\left(\omega_k - \overline{\omega}_{D0} - p\omega_\theta\right). \tag{A.1}$$

Now we want to compare the growth rate in NOVA and in Kaufman's normal mode theory, in order to be able to relate their respective mode structure information (G and $\alpha_{\mathbf{l}}$) and build a quasi-linear theory based on that. Using $\delta K_k = \omega_k^2 \int \rho \left|\boldsymbol{\xi}_k\right|^2 \mathrm{d}\mathbf{r}$, the comparison leads to $\frac{M\mathcal{E}\omega_k}{\sqrt{2}} \sum_m G_{mp} = \int d^3x \mathbf{e}_k\left(\mathbf{x}, \omega_k\right) \cdot \mathbf{j}_{\mathbf{l}}{}^k\left(\mathbf{x} \mid \mathbf{J}\right) = \frac{\omega_k}{i} V_{\mathbf{l}}$ or, alternatively

$$\alpha_{\mathbf{l}}\left(\mathbf{J}\right) = \left(\frac{M\mathcal{E}\omega_k}{\sqrt{2}}\right)^2 \sum_{m,m'} G^*_{m'p} G_{mp} = \omega_k^2 \left|V_{\mathbf{l}}\right|^2 \tag{A.2}$$

where

$$V_{\mathbf{l}} = \frac{iz}{\omega_k} \int \frac{d^3\Theta}{(2\pi)^3} \mathbf{e}_k\left(\mathbf{r}, \omega_k\right) \cdot \mathbf{v}\left(\mathbf{J}, \boldsymbol{\Theta}\right) e^{-i\mathbf{l}\cdot\boldsymbol{\Theta}}$$

which is consistent with the expression given in [25]. The mode structure is provided in NOVA via the G matrices. They are calculated via time integration that account for the eigenmode felt by a particle in a given trajectory. A weighted integration is performing according to how much time a particle spends at each position of its trajectory. Mirror-trapped particles have their parallel velocity reversed at the tips of a banana orbit, where they tend to remain longer and consequently the local mode structure will have an important contribution for the overall integration. By using equation (A.2) we can now express the quasi-linear diffusion equation, (2) and (3), in terms of NOVA code notation.

Appendix B. Expected saturation levels from a single mode perturbation theory

For a single, isolated mode in a simplified bump-on-tail situation, at the saturation ($\gamma_L \simeq -\gamma_d$, $\partial f/\partial t = 0$), we have

$$\frac{\pi}{2}\omega_{b,\mathbf{l}}^4 \mathcal{F}_{\mathbf{l}} \frac{\partial f}{\partial \Omega_{\mathbf{l}}} + \nu_{scatt,\mathbf{l}}^3 \frac{\partial (f - f_0)}{\partial \Omega_{\mathbf{l}}} = 0.$$

Analytic results far from and close to marginal stability can be used to lead the choice of the broadening parameters [15, 16]. For the case of a flat-topped window function, $\mathcal{F}_{\mathbf{l}} = 1/\Omega_{\mathbf{l}}$, we have

$$\Delta\Omega_{\mathbf{l}} = \frac{\pi}{2} \frac{\omega_{b,\mathbf{l}}^4}{\nu_{scatt,\mathbf{l}}^3} \frac{-\gamma_{d,k}}{\gamma_{L,0,k} + \gamma_{d,k}}. \tag{B.1}$$

where $\gamma_{L,0,k}$ is the initial linear growth rate.

B.1. Near marginal stability

Here close-to-marginal stability is understood in the sense that the growth rate is close to minus the damping rate, i.e. $|\gamma_{L,0,k} + \gamma_{d,k}| \ll \gamma_{L,0,k}, |\gamma_{d,k}|$. This condition implies $\omega_{b,\mathbf{l}}/\nu_{scatt,\mathbf{l}} \ll 1$ and therefore $\Delta\Omega_{\mathbf{l}} \approx c\nu_{scatt,\mathbf{l}}$. The expected saturation level from analytical theory for this case is [24, 26]

$$\omega_{b,\mathbf{l}} \simeq 1.18\nu_{scatt,\mathbf{l}} \left(\frac{\gamma_{L,0,k}}{-\gamma_{d,k}} - 1\right)^{1/4},$$

which, when substituted in (B.1) leads to $a = 2.7$.

B.2. Far from marginal stability This is the case when the initial growth rate is much larger than the damping, $\gamma_{L,0,k} \gg -\gamma_{d,k}$. For this case $\Delta\Omega_{\mathbf{l}} \approx a\omega_{b,\mathbf{l}}$. The expected saturation level from analytical theory for the case $\omega_{b,\mathbf{l}}/\nu_{scatt,\mathbf{l}} \gg 1$ is [26, 40]

$$\omega_{b,\mathbf{l}} \simeq 1.2\nu_{scatt,\mathbf{l}} \left(\frac{\gamma_{L,0,k}}{-\gamma_{d,k}}\right)^{1/3},$$

which, when substituted in (B.1) leads to $c = 2.5$. There are no known analytical solutions to rely on in order to determine the constant b. It was simply taken equal to c in previous works [11, 12, 15, 16]. We have verified that the saturation levels obtained numerically with RBQ are not sensitive with respect to the exact value of b. This is because as the mode starts its growth, the term $c\nu_{scatt,\mathbf{l}}$ has been observed to be the dominant broadening component for practical cases, as inferred by NOVA-K. On the other hand, as the mode approaches saturation, the term $a\omega_{b,\mathbf{l}}$ outweighs $b\left|\gamma_{L,k} + \gamma_{d,k}\right|$ since the latter approaches zero. The study of the parametric dependencies of the broadened window for realistic eigenmodes is under way [13] using the guiding-center, particle orbit following code ORBIT [31].

ORCID iDs

V.N. Duarte https://orcid.org/0000-0001-8096-7518
M. Podesta https://orcid.org/0000-0003-4975-0585

References

[1] Gorelenkov N.N., Pinches S.D. and Toi K. 2014 *Nucl. Fusion* **54** 125001
[2] Duarte V.N. 2017 Quasilinear and nonlinear dynamics of energetic-ion-driven Alfvén eigenmodes *PhD Thesis* University of São Paulo, Brazil (www.teses.usp.br/teses/disponiveis/43/43134/tde-01082017-195849/en.php)
[3] Collins C.S., Heidbrink W.W., Austin M.E., Kramer G.J., Pace D.C., Petty C.C., Stagner L., Van Zeeland M.A., White R.B., Zhu Y.B. and The DIII-D Team 2016 *Phys. Rev. Lett.* **116** 095001
[4] Heidbrink W.W. *et al* 2008 *Nucl. Fusion* **48** 084001
[5] Drummond W. and Pines D. 1962 *Nucl. Fusion* **2** 1049
[6] Vedenov A.A., Velikhov E.P. and Sagdeev R.Z. 1961 *Sov. Phys. Usp.* **4** 332
[7] Duarte V.N. *et al* 2017 *Nucl. Fusion* **57** 054001

[8] Duarte V.N., Berk H.L., Gorelenkov N.N., Heidbrink W.W., Kramer G.J., Nazikian R., Pace D.C., Podestà M. and Van Zeeland M.A. 2017 Theory and observation of the onset of nonlinear structures due to eigenmode destabilization by fast ions in tokamaks *Physics of Plasmas* **24** 122508

[9] Kaufman A.N. 1972 *Phys. Fluids* **15** 1063

[10] Chirikov B. 1960 *J. Nucl. Energy* C **1** 253

[11] Berk H.L., Breizman B.N., Fitzpatrick J. and Wong H.V. 1995 *Nucl. Fusion* **35** 1661

[12] Berk H.L., Breizman B.N., Fitzpatrick J., Pekker M.S., Wong H.V. and Wong K.L. 1996 *Phys. Plasmas* **3** 1827

[13] Meng G., Gorelenkov N.N., Duarte V.N., Berk H.L., White R.B. and Wang X 2018 *Nucl. Fusion* **58** 082017

[14] Fitzpatrick J. 1997 A numerical model of wave-induced fast particle transport in a fusion plasma *PhD Thesis* University of California, Berkeley, Berkeley, CA

[15] Ghantous K., Berk H.L. and Gorelenkov N.N. 2014 *Phys. Plasmas* **21** 032119

[16] Ghantous K. 2013 Reduced quasilinear models for energetic particles interaction with Alfvén eigenmodes *PhD Thesis* Princeton University

[17] Lilley M.K., Breizman B.N. and Sharapov S.E. 2010 Effect of dynamical friction on nonlinear energetic particle modes *Phys. Plasmas* **17** 092305

[18] Heidbrink W.W., Collins C.S., Podestà M., Kramer G.J., Pace D.C., Petty C.C., Stagner L., Van Zeeland M.A. White R.B. and Zhu Y.B. 2017 *Phys. Plasmas* **24** 056109

[19] Podestà M., Gorelenkova M.V. and White R.B. 2014 *Plasma Phys. Control. Fusion* **56** 055003

[20] Podestà M., Gorelenkova M., Gorelenkov N.N. and White R.B. 2017 *Plasma Phys. Control. Fusion* **59** 095008

[21] Goldston R.J., McCune D.C., Towner H.H., Davis S.L., Hawryluk R.J. and Schmidt G.L. 1981 *J. Comput. Phys.* **43** 61

[22] Dupree T.H. 1966 *Phys. Fluids* **9** 1773

[23] White R.B., Gorelenkov N.N., Heidbrink W.W. and Van Zeeland M.A. 2010 *Plasma Phys. Control. Fusion* **53** 045012

[24] Berk H.L. and Breizman B.N. 1990 *Phys. Fluids* B **2** 2235

[25] Berk H.L., Breizman B.N. and Pekker M.S. 1997 *Plasma Phys. Rep.* **23** 778

[26] Gorelenkov N.N., Chen Y., White R.B. and Berk H.L. 1999 *Phys. Plasmas* **6** 629

[27] Gorelenkov N.N., Cheng C.Z. and Fu G.Y. 1999 *Phys. Plasmas* **6** 2802

[28] Pankin A. *et al* 2004 *Comput. Phys. Commun.* **159** 157

[29] Podestà M., Gorelenkova M., Fredrickson E.D., Gorelenkov N.N. and White R.B. 2016 *Nucl. Fusion* **56** 112005

[30] Podestà M., Gorelenkova M., Fredrickson E.D., Gorelenkov N.N. and White R.B. 2016 *Phys. Plasmas* **23** 056106

[31] White R.B. and Chance M.S. 1984 *Phys. Fluids* **27** 2455

[32] White R.B. 2011 *Plasma Phys. Control. Fusion* **53** 085018

[33] White R.B. 2012 *Commun. Nonlinear Sci. Numer. Simul.* **17** 2200

[34] Gorelenkov N.N., Heidbrink W.W., Kramer G.J., Lestz J.B., Podestà M., Van Zeeland M.A. and White R.B. 2016 *Nucl. Fusion* **56** 112015

[35] Borba D. *et al* JET-EFDA Contributors 2010 *Proc. 23rd IAEA Fusion Energy Conf. (Daejeon, Republic of Korea, 11–16 October 2010)* IAEA-CN-180/THW/P7-08 pp 1–8 (www-pub.iaea.org/iaeameetings/38091/23rd-IAEA-Fusion-Energy-Conference)

[36] Podestà M., Gorelenkova M.V., Darrow D.S., Fredrickson E.D., Gerhardt S.P. and White R.B. 2015 *Nucl. Fusion* **55** 053018

[37] Cheng C.Z., Chen L. and Chance M.S. 1985 *Ann. Phys.* **161** 21

[38] Cheng C.Z. 1992 *Phys. Rep.* **211** 1

[39] Berk H.L., Breizman B.N. and Pekker M.S. 1996 *Phys. Rev. Lett.* **76** 1256

[40] Berk H.L. and Breizman B.N. 1990 *Phys. Fluids* B **2** 2246

[41] White R.B. 2013 *The Theory of Toroidally Confined Plasmas* 3rd edn (London: Imperial College Press)